

3D-Pharmacophore Modeling, Molecular Docking, and Virtual Screening for Discovery of Novel CDK4/6 Selective Inhibitors

Amany Belal^{a, b, 1}

^aDepartment of Pharmaceutical Chemistry, College of Pharmacy, Taif University, P.O. Box 11099, Taif, 21944 Saudi Arabia

^bMedicinal Chemistry Department, Faculty of Pharmacy, Beni-Suef University, Beni-Suef, 62514 Egypt

Received October 28, 2020; revised November 8, 2020; accepted November 10, 2020

Abstract—Structure-based pharmacophore mapping, drug-likeness and ADMET profiles were used as tools in our virtual screening process, in addition to molecular docking studies that were used to find novel CDK4/6 inhibitors with different heterocyclic scaffolds, having appropriate physicochemical parameters and non toxic. Aim of this work is to search for new promising CDK4/6 inhibitors, that have a great potential to be approved as clinically useful drugs in cancer therapy. Six promising hits were retrieved after applying virtual screening filters, these hits were subjected to molecular docking studies and were compared with the approved CDK4/6 inhibitor drug (palbociclib). Finally, we can conclude that they have a great potential to target CDK4/6 in a closely similar manner as palbociclib, in addition to their predicted good ADMET properties, they can be considered as novel hopeful leads for CDK4/6 inhibition and deserve further clinical investigations.

Keywords: lead discovery, pharmacophore, drug-like molecules, computational drug design, CDKs, molecular docking, CDK4/6

DOI: 10.1134/S1068162021330013

INTRODUCTION

Cyclin-dependent kinases (CDKs), are serine/threonine protein type kinases, they play a critical role in cell cycle regulation and transcription, there are 20 known cyclin-dependent kinases (CDKs) till the moment [1, 2]. They are involved in many biological processes such as neurogenesis, translation and apoptosis. Deregulation of CDKs will al mostly lead to oncogenesis, they are overexpressed in numerous types of cancers [3].

Cyclin-dependent kinases control the transition process of the cell from one stage to the next stage, therefore, they have been considered as promising targets for cancer treatment as uncontrolled cell growth and proliferation is usually mediated by cell-cycle dysregulation and over activation of cyclin-dependent kinases (CDKs) [4]. However, nonselective inhibition of CDKs was found to cause toxic effects for noncancer cells [5]. Selective targeting to CDKs 4 and 6 is a step to overcome toxicity issues, these two kinases are similar in function and structure, they mediate the transition process from G₀/G₁-phase to S-phase in cell cycle and control Rb/E2F transcription. CDK4/6 inhibitors are of great value in treatment of different

types of cancers as melanoma, breast cancer, osteosarcoma, skin cancer, bladder cancer, lung cancer and stomach cancer, CDK4/6 perform phosphorylation to RB1 and RB1-like protein 1 (p130) and RB1-like protein 2 (p107), so they are considered as valuable and selective targets in cancer therapy [6].

The three FDA approved drugs abemaciclib, palbociclib and ribociclib (Fig. 1), [4], that acts as CDK4/6 inhibitors and have shown remarkable anticancer activity with manageable toxic effects. They proved to be able in targeting tumors, in which CDK4/6 has a pivotal role in the G₁-to-S-phase cell-cycle transition, with improved efficacy and fewer side effects. Only these three drugs are approved as selective CDK4/6 inhibitors till now, so we are still in the need for discovery of new selective molecules that can act against CDK4/6 with minimal or no side effects.

CADD and virtual screening of databases are widely used to help in drug design, drug development and drug discovery. They are considered as an important and useful tools in finding new lead structures for treatment of diseases. Using these in silico techniques can reduce time and costs by millions of dollars to discover new active molecules. Pharmacophore modeling is a succefully applied method in drug discovery, it can reduce the complexity of several structural fea-

¹ Corresponding author: e-mail: a.belal@tu.edu.sa; amanybelal2010@gmail.com.

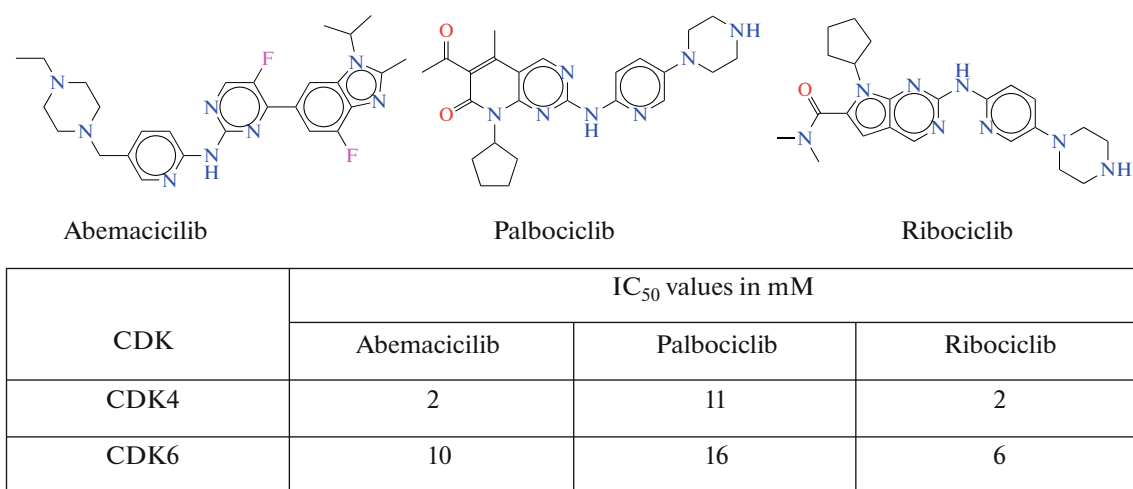


Fig. 1. FDA approved CDK4/6 inhibitors.

tures to a set of few features [7–9]. In this research work we used molecular modeling methodologies to help us search for new selective CDK4/6 inhibitors with better pharmacokinetic properties. Pharmacophore model was built using the FDA actually approved drugs (Fig. 1). CDK4/6 inhibitors collected from data bases [10–15] were used as test set to assure the ability of the generated model in identifying CDK4/6 inhibitors, further filtration steps were performed as drug-likeness and ADMET profile filters. Finally, six hits were selected, with promising activity and good ADMET properties. Molecular docking was used as a tool in this work to explore the binding modes of these hits, their affinity and other possible interactions with CDK4 and CDK6. All these investigations revealed that these six hits can be considered as novel hopeful leads for CDK4/6 inhibition and can be subjected for further investigation as they proved to have good promiscuity to be approved as selective CDK4/6 inhibitor drugs.

RESULTS AND DISCUSSION

Structure-Based Pharmacophore Generation and Validation

The three approved CDK4/6 inhibitors palbociclib, abemaciclib and ribociclib (training set), were subjected to flexible alignment before creating the structure based pharmacophore query using MOE software (Chemical Computing Group, Montreal, Canada) package [16]. Which has proved to be an effective tool for generating pharmacophore queries [17]. Figure 3 is showing that the backbones of these three compounds have structure similarity and they are aligned well with each other, then the PPCH_All scheme in MOE software was used to construct the pharmacophore model. Eight features were generated,

they were checked to match all drugs through switching essential and ignore functions on/off, till obtaining that there are five features proved to be essential for the three molecules, these features (Fig. 4) were then saved as the ph4 file. The five necessary features as represented in Fig. 5 and (VA) (with distances) are F1: hydrogen bond donor, F2: hydrogen bond acceptor/metal ligator, F3: hydrophobic area, F4: hydrophobic planar area (sp^2)/ hydrophobic non planar area (sp^3) and F5: metal ligator/hydrophobic area/ hydrogen bond acceptor. This query was further validated through detecting its ability to identify the active hits, a series of reported potent and selective inhibitors for CDK4/6 were obtained (Fig. 2) from the literature [10–15], the pharmacophore query showed the ability to identify all of them as being active. Matching between aligned molecules of the test set compounds in addition to the three approved drugs (Fig. 5b) with the generated pharmacophore query is shown in Fig. 6.

Virtual Screening: Pharmacophore-Based Database Screening

ChEMBL data base [18] was used for this purpose through structure similarity search using smiles to get compounds with more than 80% similarity with palbociclib. The obtained data base composed of 510 compounds of diverse chemical structures with a close similarity to palbociclib was downloaded as sdf then treated with MOE for further analysis against the pharmacophore generated query. 141 hits out of 510 revealed to have all the necessary features in the generated query.

Drug-likeness analysis. Compounds that obey Lipinski rule of five (RO5) are likely to be orally active molecules with a great potential of being drug like

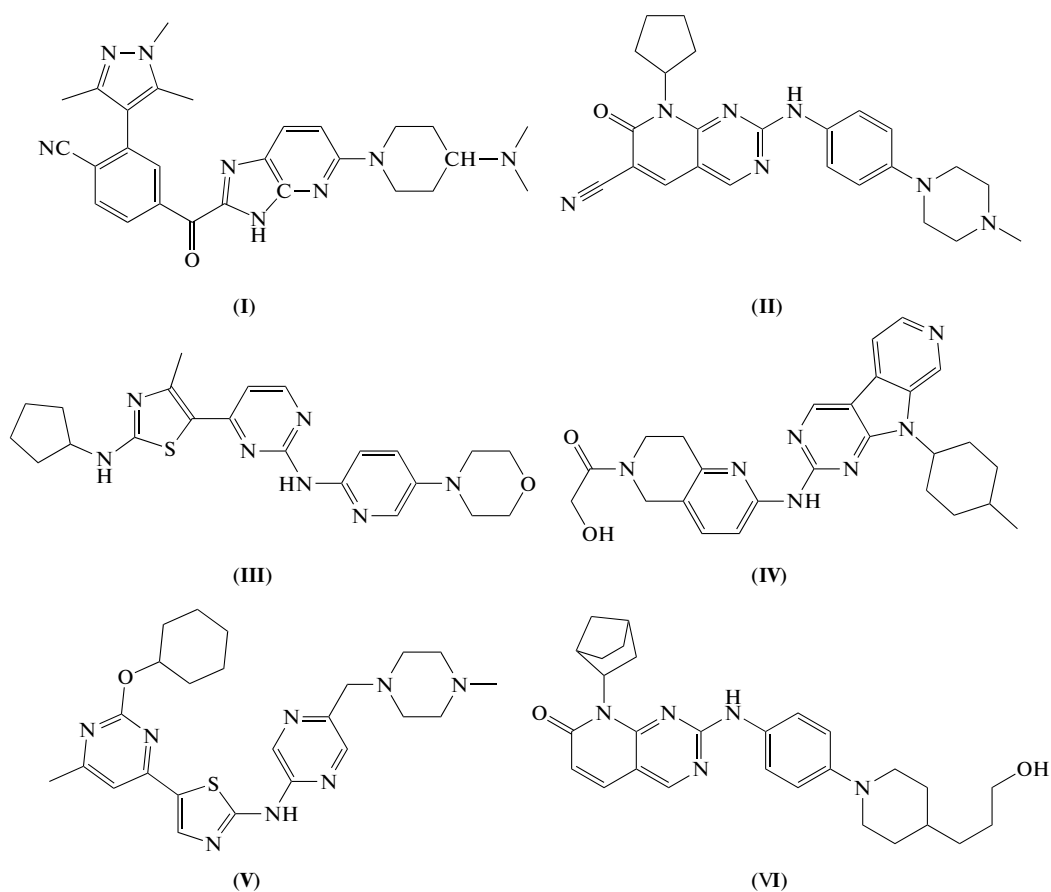


Fig. 2. 2D structures of the test set compounds.

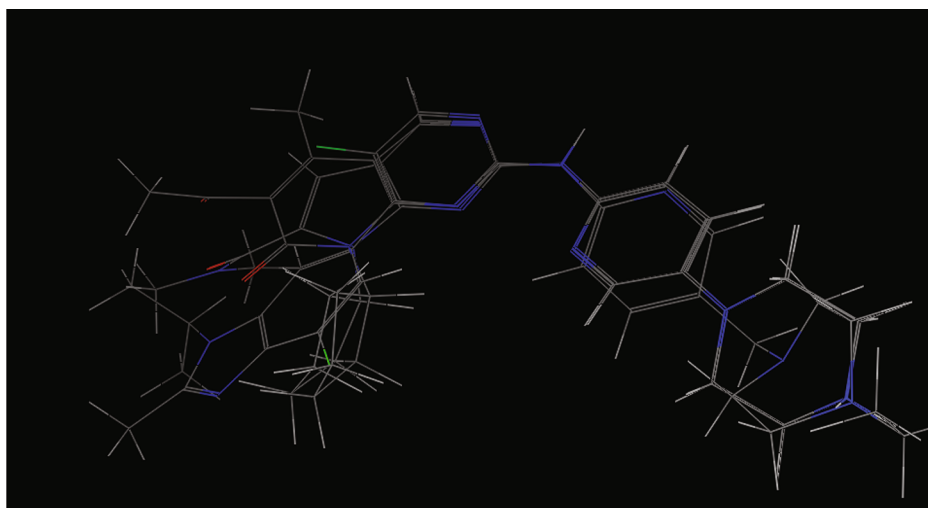


Fig. 3. Aligned FDA approved CDK4/6 inhibitors (Palbociclib, ribociclib and abemaciclib).

compounds [19]. The retrieved 141 diverse molecules obtained from ChEMBL data base and obey the validated query was then filtered using RO5, only molecules that are compatible with this rule are selected for

further screening. 37 hits were chosen after performing the filtration step.

ADMET analysis. Compounds that have promiscuity of being active inhibitors according to their satis-

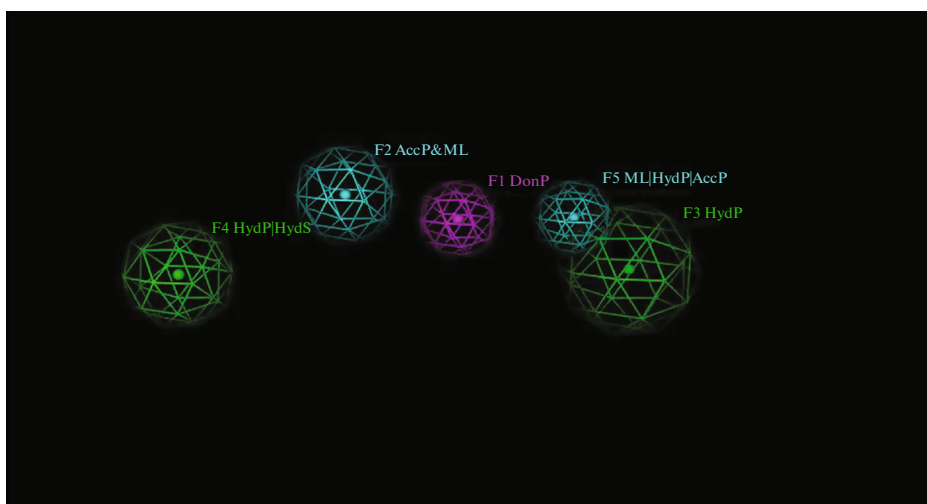


Fig. 4. The generated pharmacophore query, with the 5 essential features in FDA approved drugs.

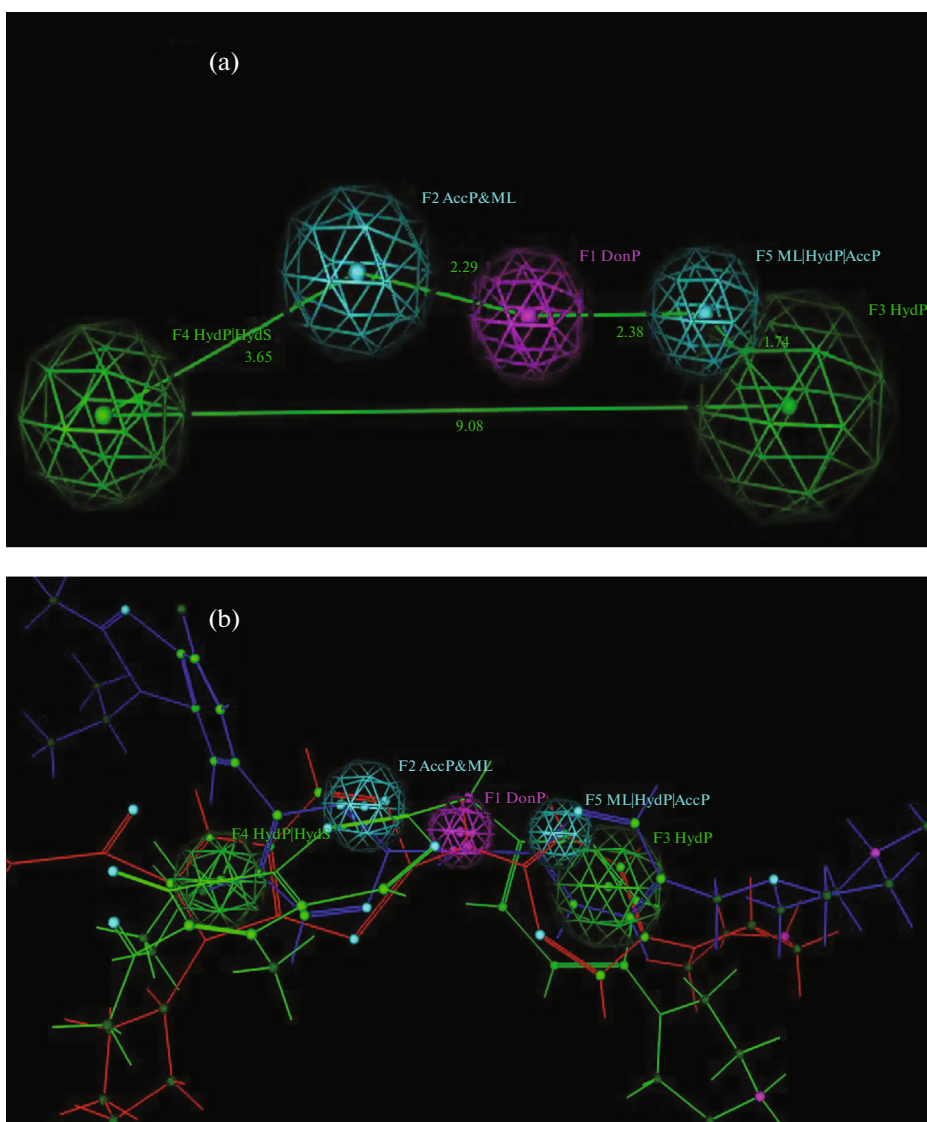


Fig. 5. (a) PPCH-All query with distances. (b) Mapping of the PPCH-All query with the three drugs: abemaciclib (blue), ribociclib (red), palbociclib (green).

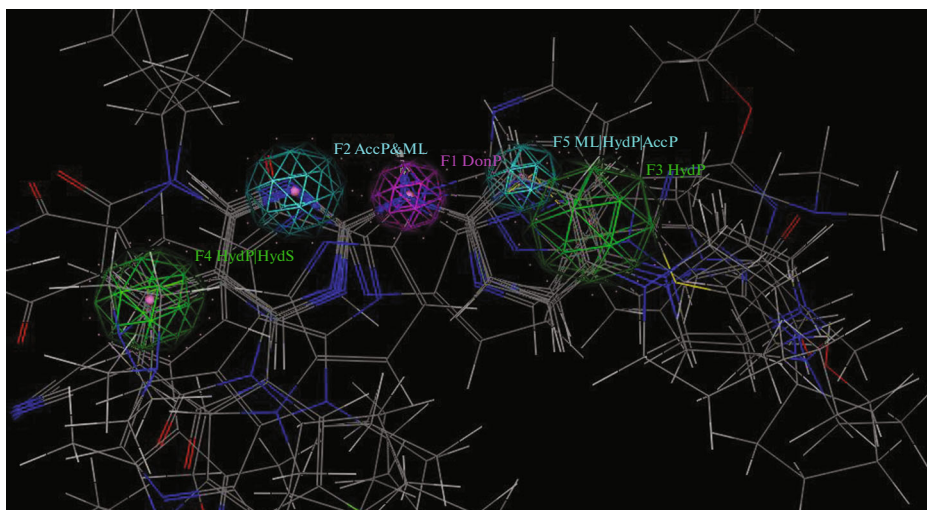


Fig. 6. FDA approved drugs and test set compounds aligned and mapped with the pharmacophore model.

fraction to all features of the pharmacophore query, but they have bad ADMET properties will have problems if they subjected for further in vivo experiments. This proves the importance of studying the ADMET (absorption, distribution, metabolism, elimination, toxicity) analysis as a crucial step in drug design. Molecules that are predicted to penetrate BBB, to be absorbed from human intestine, low CYP inhibitory promiscuity, non AMES toxic and non carcinogenic will be selected as promising hits for further investigations. After applying these restrictions using ADMET-SAR tool [20], only 6 hits (Table 1) are satisfactory with these conditions.

Molecular docking studies: The retrieved 6 hits (Table 1) and palbociclib were drawn in their 2D forms saved as mol, then treated with MOE software and saved as mdb for docking into the binding site of both CDK4 (pdb: 2W9Z) [21] and CDK6 (pdb: 5L2I) [22]. As for binding affinity, all 6 hits revealed better or comparable score with palbociclib in both CDK4/6, the range of docking score of the 6 hits into CDK4 and palbociclib was (−21.34 to −16.1) and −18.16 kcal/mol respectively. (−24.03 to −17.46) was the range of docking score for the 6 hits inside CDK6 and −21.58 kcal/mol for palbociclib (Table 2).

Inspection of the 2D interactions was performed, all compounds fitted well in the binding site and their interactions was described (Table 2), in addition 2D and 3D binding interactions are shown in Figs. 7–14 and Suppl. Data, it is noticed that palbociclib formed two hydrogen bonding with Val101 and one hydrogen bonding with Asp163 in ATP binding site of CDK6 in addition to ligand exposure through its piperazine moiety. Compounds (VII) and (VIII) like palbociclib showed ligand exposure and two hydrogen bonding

with Val101, additionally, they showed arene–arene interaction with Phe98 amino acid, Figs. 7–9 representing 2D and 3D binding of compounds (VII) and (VIII) and palbociclib inside CDK6 binding site and alignment of these two promising molecules (VII) and (VIII) with palbociclib inside the binding site of CDK6 is also shown in Fig. 10. The other four hits also showed ligand exposure (sup. data) and interactions with amino acids but these amino acids are different from that interacted with palbociclib, hit (IX), showed arene–arene interaction with Phe98, hit (X), revealed two hydrogen bonding with Asp104, hit (XI) showed hydrogen bonding with Lys43 and hit (XII) with Lys29. Additionally both hits (X) and (XI) formed another hydrogen bonding with Asp163 like palbociclib. This results indicates the promiscuity of these hits in comparison to the approved drug palbociclib. Alignment of the other hits (IX–XII) with palbociclib inside CDK6 ATP binding site are presented in the sup. Data. Files.

Docking of palbociclib and the retrieved 6 hits into CDK4 binding site was performed using MOE software, 2D and 3D interactions are represented in Figs. 11–13 and the additional figures can be seen in the sup. Data files. Palbociclib showed two interactions with Glu94 and Lys35 as hydrogen bonding and arene–cation respectively, in addition to ligand exposure. All the docked hits showed possible interaction with Lys35 amino acid as palbociclib. Additional interactions and ligand exposure are also expressed by the retrieved hits inside CDK4 binding site, hit (VIII) showed possible arene–cation interaction with Arg101 and another hydrogen bond with Lys211, hit (IX) showed two hydrogen bonding with Lys95 and Val96, hit (X) showed arene–cation interaction with Arg101.

Table 1. The final promising 6 hits with their ChEMBL and Zinc data base codes

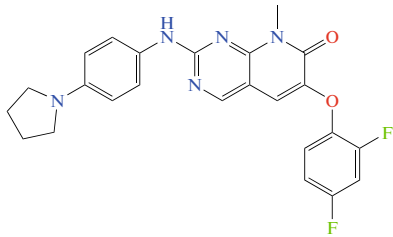
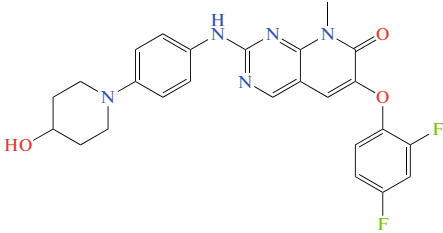
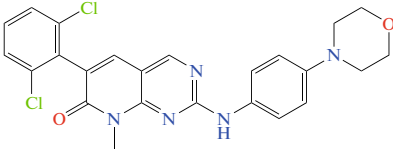
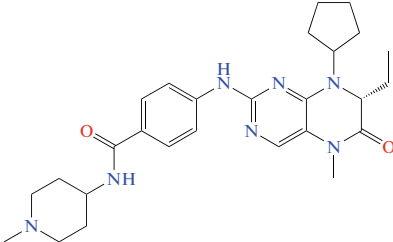
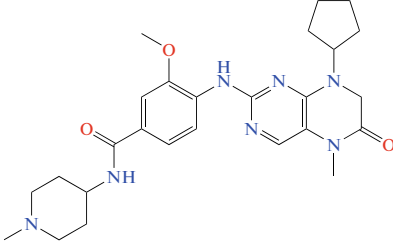
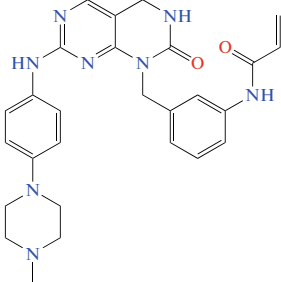
No.	ChEMBL code	ZINC code	Structure
(VII)	CHEMBL3746117	ZINC653799671	
(VIII)	CHEMBL3746959	ZINC653799671	
(IX)	CHEMBL106772	<u>ZINC000013812765</u>	
(X)	CHEMBL3609309	<u>ZINC000003986141</u>	
(XI)	CHEMBL3609304	<u>ZINC000473083535</u>	
(XII)	CHEMBL3601726	<u>ZINC000473085995</u>	

Table 2. Docking scores and types of interactions for the retrieved six hits

Comp. No.	Docking Score, kcal/mol		Types of interactions	
	CDK4	CDK6	CDK4	CDK6
(VII)	-20.37	-22.32	Arene cation with Lys35	2 HB with Val101 and arene–arene interaction with Phe98
(VIII)	-16.1	-19.94	HB with Lys35, arene cation with Arg101, HB with Lys211	2 HB with Val101 and arene–arene interaction with Phe98
(IX)	-17.44	-17.46	2 HB with Lys95, Val 96 and arene cation with Lys35	Arene–arene interaction with Phe98
(X)	-18.95	-21.55	HB with Lys35 and arene cation with Arg101	HB with Asp104 and HB with Asp163
(XI)	-19.78	-24.03	HB with Lys35	HB with Lys43 and HB with Asp163
(XII)	-21.34	-23.75	2 HB with Lys35 and arene cation with Arg101	HB with Lys29
Palbociclib	-18.16	-21.58	HB with Glu94 and arene cation with Lys35	2 HB with Val101 and 1 HB with Asp163

Hit (XII) showed not only one interaction with Lys35, but it showed ability to form two hydrogen bonding with this amino acid, in addition to arene-cation interaction with Arg101 amino acid. Pharmacophore mapping of the final 6 hits are represented in Fig. 15.

Overview, future perspectives and availability of the hopeful molecules. The common 2D features between the 6 hits are aromatic pyrimidine fused with a six membered ketonic heterocyclic moiety (contain one or two nitrogen atoms), the NH group as spacer between the fused pyrimidine and a phenyl moiety, the phenyl moiety is almostly substituted at the para position with secondary amine, additional hydrophobic moiety is attached to the fused pyrimidine system at different positions as shown in Fig. 16, which represent a simplified and helpful diagram for designing new CDK4/6 inhibitors.

As for our retrieved six hits, their ChEMBL and Zinc data base codes are represented in Table 2, hit (VII) and (VIII) [23] were synthesized in 2016 by Laura et al for treatment of diabetes. Hit (IX) was screened in 2000 by Alan et al. [24] as tyrosine kinase inhibitor. Hits (X) and (XI) [25] were screened by Lijia et al. in 2015 for BBD4 and PLK1 inhibitory activity. Finally hit (XII) [26] was designed in 2015 by Tan et al. as JAK3 inhibitor. However, in this research work we can put a clear evidence for the usefulness of these 6 hits as CDK4/6 inhibitors with a great promiscuity to be approved as clinically useful drugs as palbociclib.

CONCLUSION

In this Research work, structure based pharmacophore model was built and used to search for novel and potent CDK4/6 inhibitors. The generated PPCH-All

pharmacophore query is composed of five chemical features produced automatically using MOE software after performing alignment of the approved CDK4/6 inhibitor drugs. This model was validated for its ability to identify chemical compounds that were reported as CDK4/6 inhibitors. The reliable pharmacophore query was used to screen a library of 510 compounds, obtained from ChEMBL data base. 141 Hits are shown to match all the generated five features. Further filtrations were performed by using Lipinski parameters and ADMET profile. Finally, six hits were obtained after performing all the previous steps, then molecular docking studies were performed for these hits to investigate the possible interactions between these hopeful hits and CDK4/6. After performing these studies we can conclude that, these six hits can be considered as leads against CDK4/6 and have a great potential to be subjected to further clinical investigations hopefully to be approved as drugs in the future.

EXPERIMENTAL

Pharmacophore generation and validation. 3D structures of the following drugs: palbociclib, abemaciclib and ribociclib were built by MOE [16] after getting their smiles from pubchem [27], protonated and energy minimized using MMFF94x force field. Data base for these drugs was established and saved as mdb file. The pharmacophore query was built after performing alignment of the minimized structures of the saved previous drugs. After alignment, the lowest s value was used for generating the pharmacophore mapping. PPCH-All option was used for building up the mapping process, the generated features were

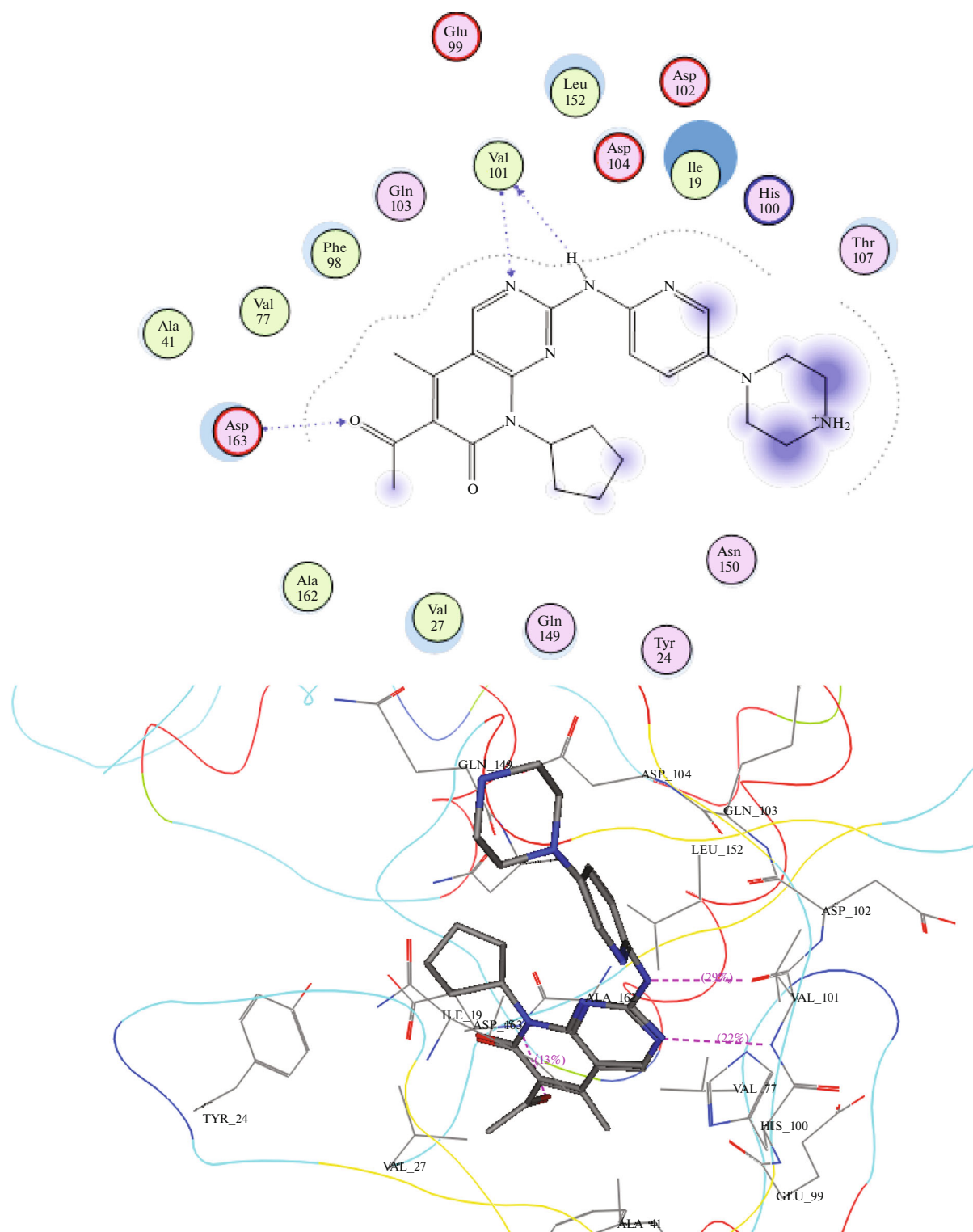


Fig. 7. 2D and 3D interactions of palbociclib in CDK6 binding site.

screened one by one using ignore and essential options to help fix only the features that are present in the three mentioned drugs (training set), finally we get a

five shared features between them, these obtained final essential and common features were saved as ph4 file and it was validated by test set molecules and

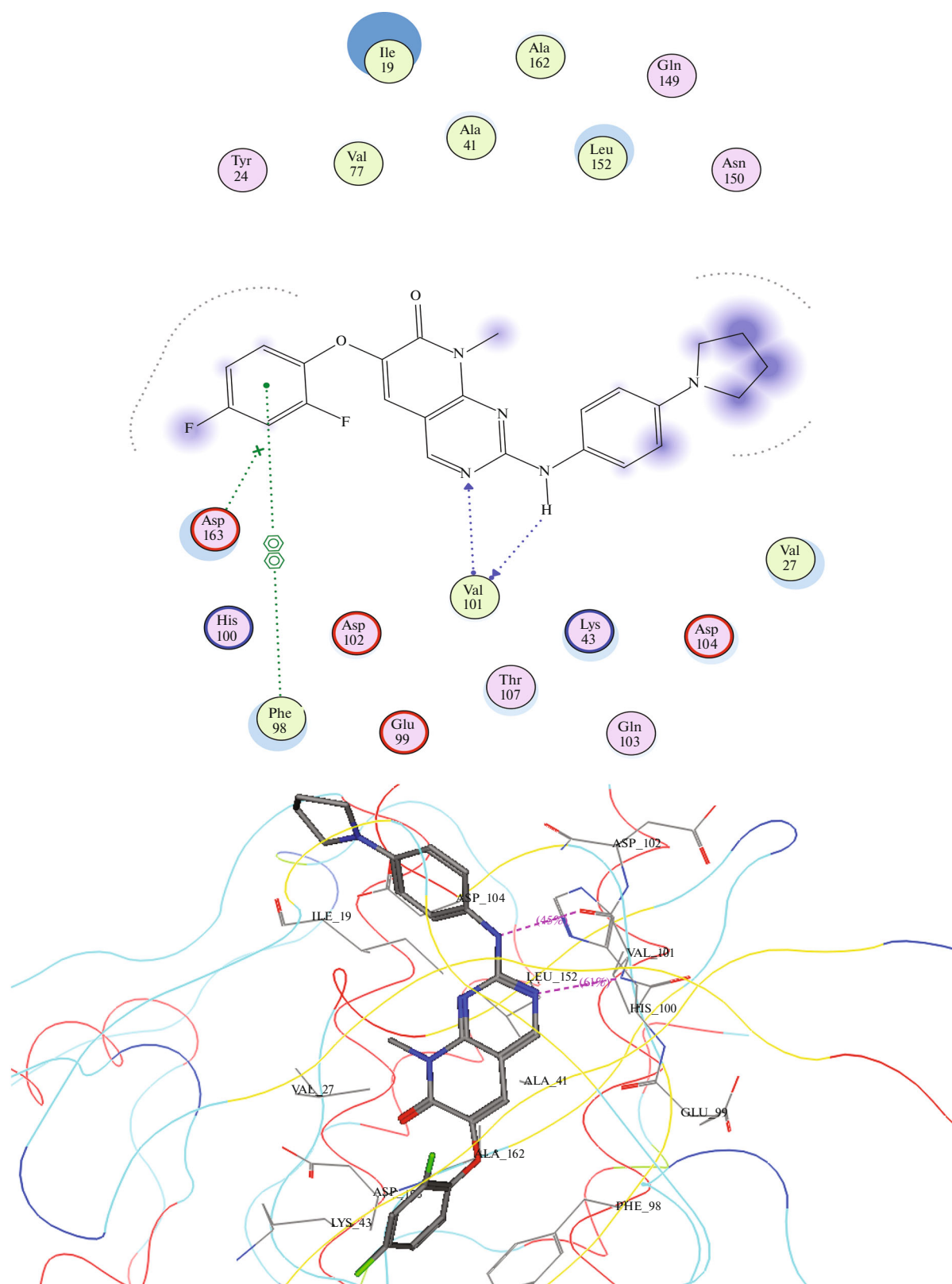


Fig. 8. 2D and 3D interactions of compound (VII) in CDK6 binding site.

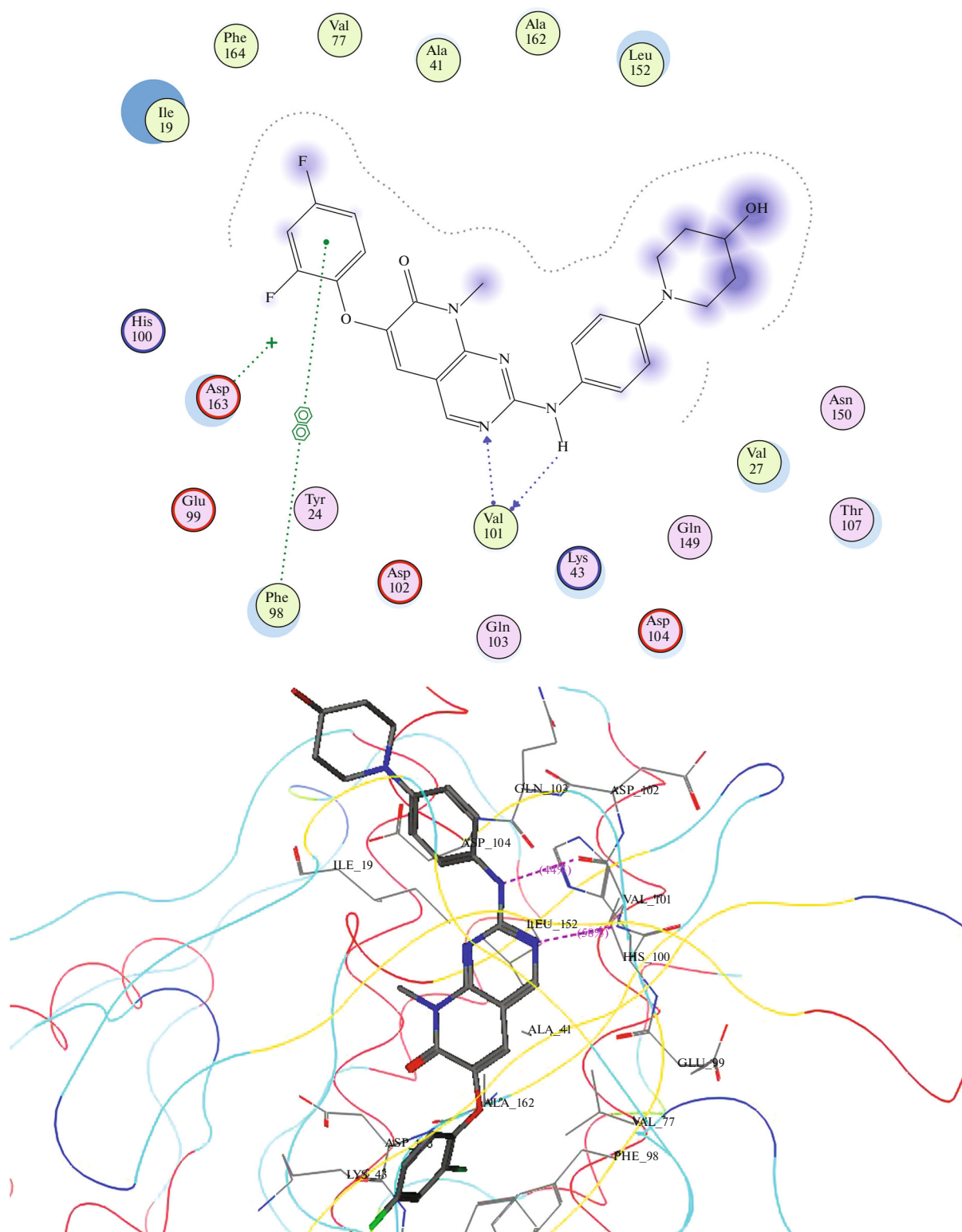


Fig. 9. 2D and 3D interactions of compound (VIII) in CDK6 binding site.

revealed to be able to identify all of them. It is now ready to be used against libraries of different molecules by keeping all the default options of MOE software.

Virtual screening. Virtual screening is used in this study to find different scaffolds promising to act as potential leads with CDK4/6 inhibitory properties.

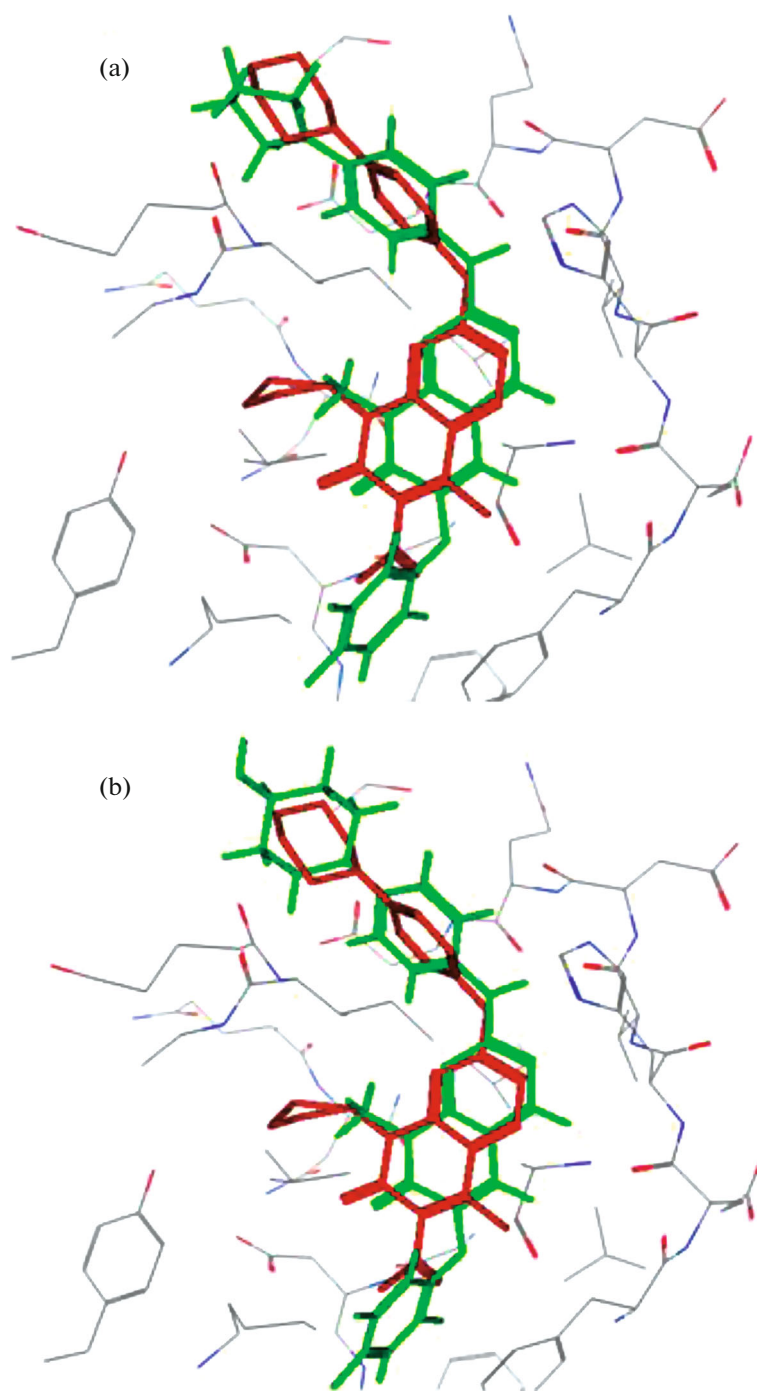


Fig. 10. (a) Alignment bet. palbociclib (red) and compound (VII). (b) Alignment bet palbociclib (red) and compound (VIII) in CDK6 binding site.

The first step is downloading a data base of 510 compounds from ChEMBL by searching for compounds with more than 80% similarity with palbociclib. The downloaded data base was saved as mdb using MOE software, then screened against the generated and validated pharmacophore query. 141 Hits were found to satisfy all query features.

Drug-likeness and ADMET analysis. The filtered molecules then subjected to lipinski filter, to exclude any molecules that disobey lipinski parameters. Thirty seven hits were retrieved, then checked using ADMET-SAR [20] for their ADMET profile. Finally 6 hits were retrieved. The compounds that fitted to all the features of the structure-based pharmacophore

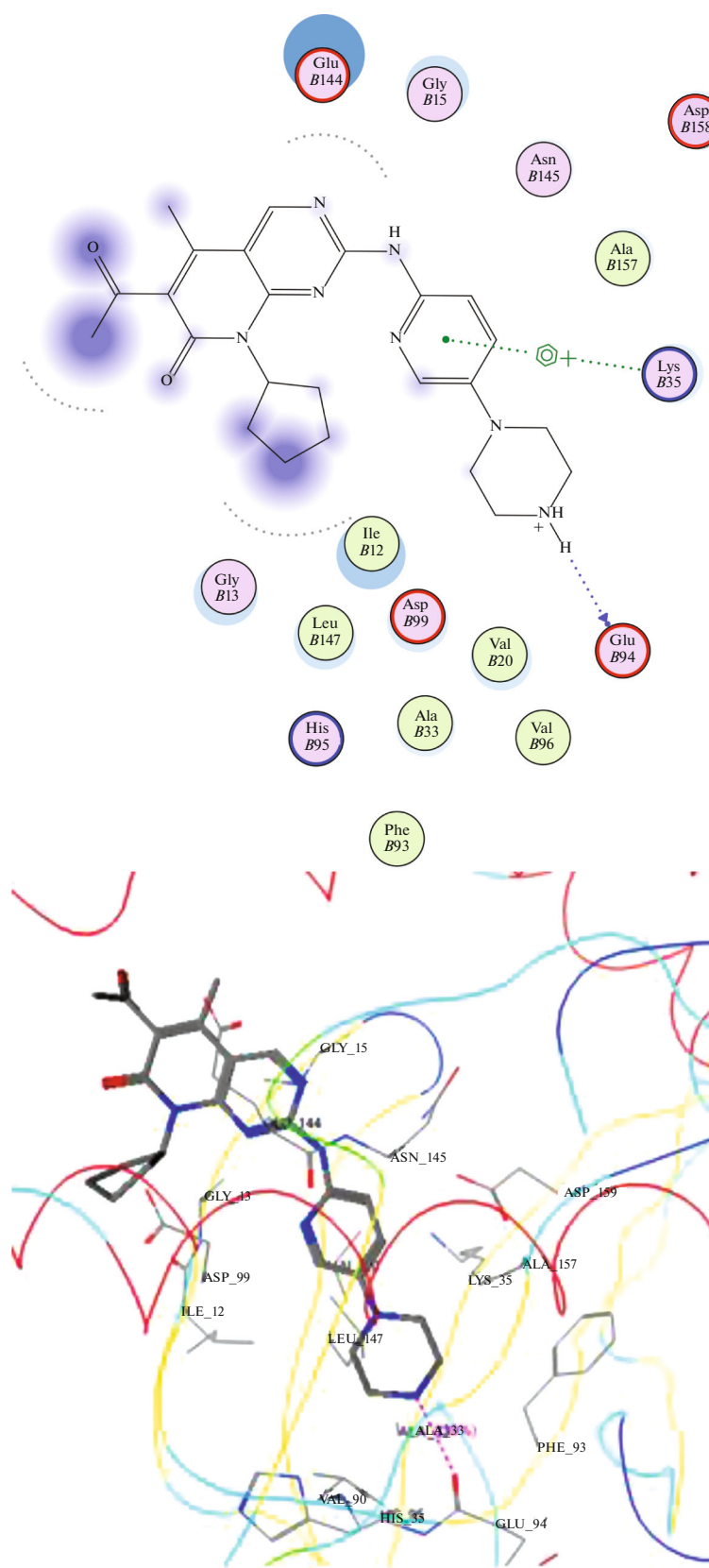


Fig. 11. 2D and 3D interactions of palbociclib in CDK4 binding site.

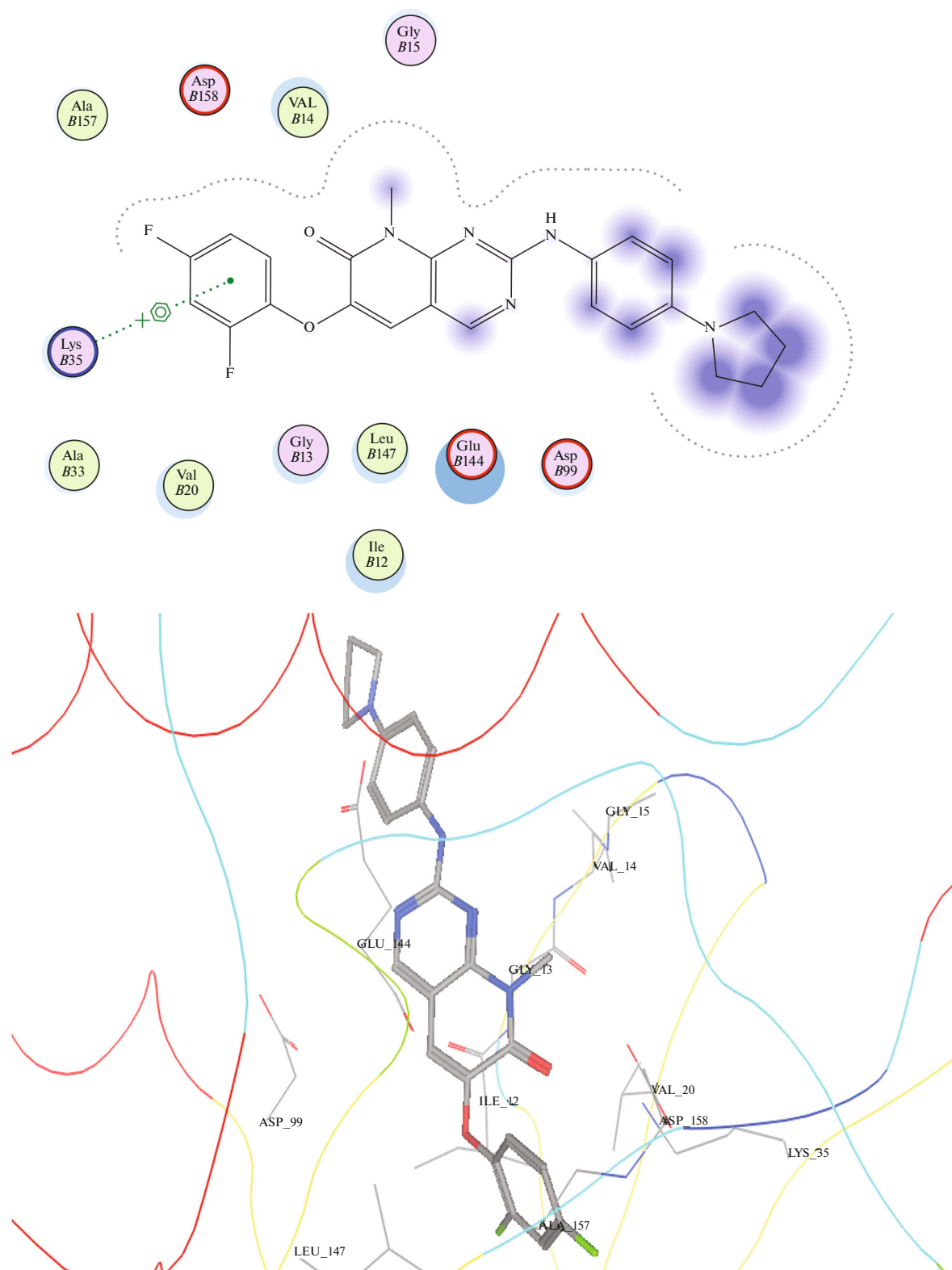


Fig. 12. 2D and 3D interactions of compound (VII) in CDK4 binding site.

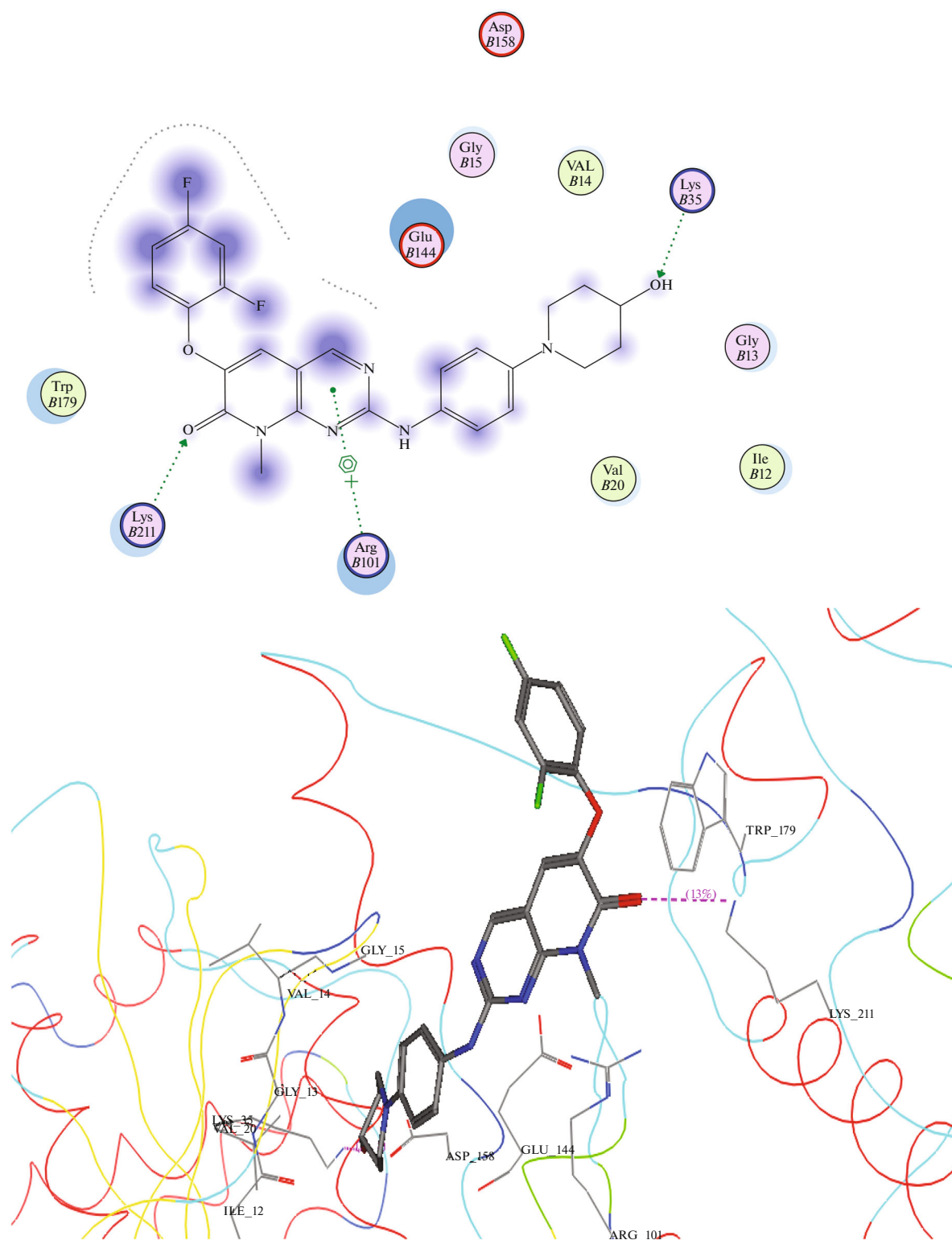


Fig. 13. 2D and 3D interactions of compound (VIII) in CDK4 binding site.

model were picked up, further filtration by Lipinski's rule, then, ADMET (absorption, distribution, metabolism, elimination, toxicity) profile. The hits that sat-

isfy Lipinski's rule and all pharmacophoric features in the generated model, having good ADMET properties and predicted to have good profile will be only considered.

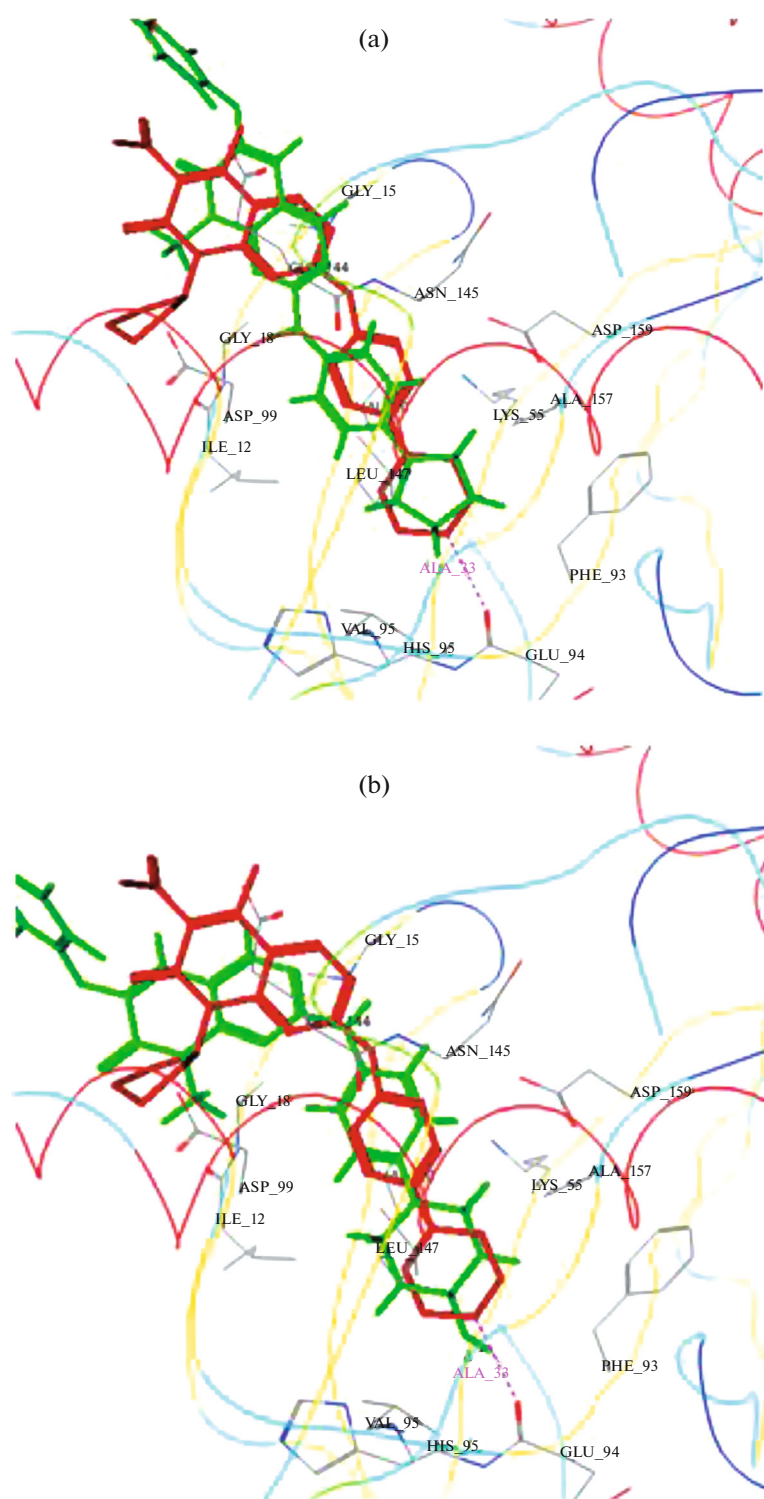


Fig. 14. (a) Alignment bet. palbociclib (red) and compound (VII). (b) Alignment bet palbociclib (red) and comp. (VIII) in CDK4 binding site.

Molecular docking studies. Pdb files for CDK4 (pdb: 2W9Z) [21] and CDK6 (pdb: 5L2I) [22] were downloaded from protein data bank according to the

mentioned pdb ID, hydrogen atoms were added, water chains were removed, then subjected to energy minimization using MMFF94x force field. Binding site

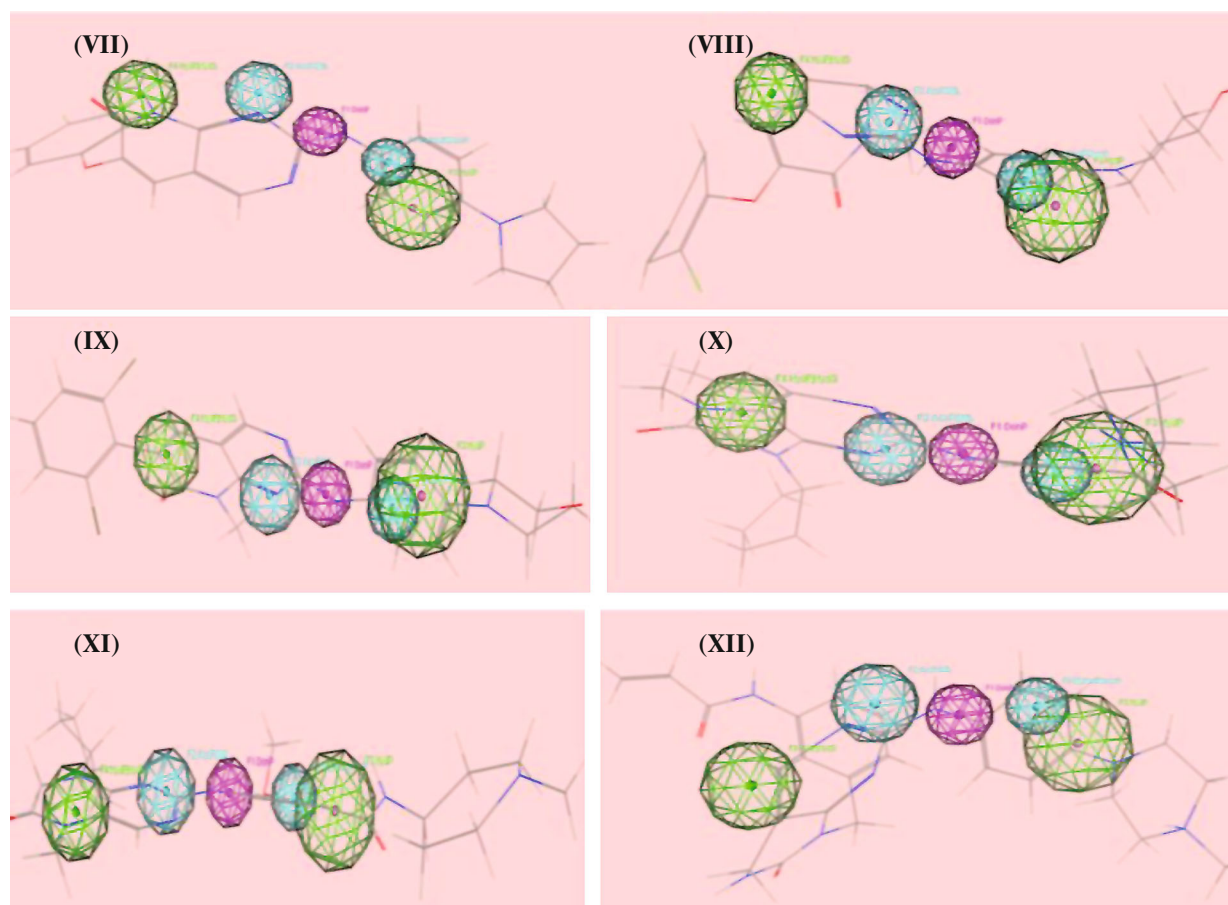


Fig. 15. Mapping of our 6 hits with PPCH-All pharmacophore query.

was detected using site finder option fixed in MOE software and then saved as Moe file. Palbociclib and the six hits 2D structures were converted to 3D by MOE, protonated and energy minimized using 0.05 gradient, MMFF94X Force Field, with RMS gradient of 0.05 and the the LowModMD method was applied to choose the conformers with the lowest energy, then

saved as mdb file for docking. Docking simulation was performed using MOE and conformers with the lowest S value were chosen, ligand interaction option was used to visualize and inspect 2D interactions between the docked poses and the perspective binding site. All the obtained data are tabulated (Table 2) and pictured in Figs. 7–14 and Suppl. Data files.

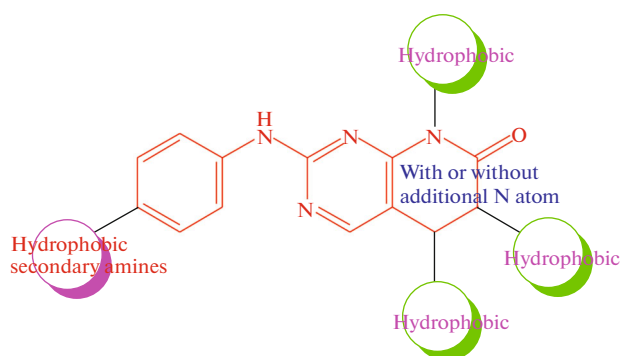


Fig. 16. 2D structural features for the six hits: The common skeleton colored in red and different positions for other substituents as labeled.

ACKNOWLEDGMENT

Appreciated thanks to Taif University Researchers Supporting Project number (TURSP-2020/35), Taif University, Taif, Saudi Arabia.

FUNDING

This work was financially supported by Taif University Researchers Supporting Project number (TURSP-2020/35), Taif University, Taif, Saudi Arabia.

COMPLIANCE WITH ETHICAL STANDARDS

No experiments have been conducted on humans or animals in this research work.

Conflict of Interests

The authors declare that there is no conflict of interest.

SUPPLEMENTARY INFORMATION

The online version contains supplementary material available at [10.1134/S1068162021330013](https://doi.org/10.1134/S1068162021330013).

REFERENCES

- Malumbres, M., *Genome Biol.*, 2014, vol. 15, pp. 1–10. <http://genomebiology.com/2014/15/6/122>.
- Harper, J. and Adams, P., *Chem. Rev.*, 2001, vol. 101, pp. 2511–2526.
- Ding, L., Cao, J., Lin, W., Chen, H., Xiong, X., Ao H., Yu M., Lin J., Cui Q. *Int. J. Mol. Sci.* 2020, vol. 21, p. 1960. <https://doi.org/10.3390/ijms21061960>
- Sourav, K., Gaurav, J., Anjana, M., and Raj, K., *Eur. J. Med. Chem.*, 2017, vol. 142, pp. 424–458.
- Neil, J. and Geoffrey, I.S., *Expert Opin. Ther. Targets*, 2010, vol. 14, pp. 1199–1212.
- Aggarwal, P., Vaites, L.P., Kim, J.K., Mellert, H., Gurrung, B., Nakagawa, H., Herlyn, M., Hua, X., Rustgi, A.K., and McMahon, S.B., *Cancer Cell*, 2010, vol. 18, pp. 329–340.
- Ugale, V.G. and Bari, S.B., *SAR QSAR Environ. Res.*, 2016, vol. 27, pp. 125–145.
- Meetei, P.A., Rathore, R.S., Prabhu, N.P., and Vindal, V., *Springer Plus*, 2016, vol. 5, p. 965.
- Tuccinardi, T., Poli, G., Corchia, I., Granchi, C., Lapillo, M., Macchia, M., Minutolo, F., Ortore, G., and Martinelli, A., *Mol. Inform.*, 2016, vol. 35, pp. 434–439.
- Cho, Y.S., Angove, H., Brain, C., Chen, C.H., Cheng, H., Cheng, R., Chopra, R., Chung, K., Congreve, M., Dagostin, C., Davis, D.J., Feltell, R., Giraldez, J., Hiscock, S.D., Kim, S., Kovats, S., Lagu, B., Lewry, K., Loo, A., Lu, Y., Luzzio, M., Maniara, W., McMenamin, R., Mortenson, P.N., Benning, R., O'Reilly, M., Rees, D.C., Shen, J., Smith, T., Wang, Y., Williams, G., Woolford, A.J., Wrona, W., Xu, M., Yang, F., and Howard, S., *ACS Med. Chem. Lett.*, 2012, vol. 17, pp. 445–449.
- Reddy, M.V., Akula, B., Cosenza, S.C., Athuluridivakar, S., Mallireddigari, M.R., Pallela, V.R., Billa, V.K., Subbaiah, D.R., Bharathi, E.V., Vasquez-Del Carpio, R., Padgaonkar, A., Baker, S.J., and Reddy, E.P., *J. Med. Chem.*, 2014, vol. 13, pp. 578–599.
- Tadesse, S., Yu, M., Mekonnen, L.B., Lam, F., Islam, S., Tomusange, K., Rahaman, M.H., Noll, B., Basnet, S.K., Teo, T., Albrecht, H., Milne, R., and Wang, S., *J. Med. Chem.*, 2017, vol. 9, pp. 1892–1915.
- Tadesse, S., Yu, M., Kumarasiri, M., Le, B.T., and Wang, S., *Cell Cycle*, 2015, vol. 14, pp. 3220–3230.
- Hirai, H., Shimomura, T., Kobayashi, M., Eguchi, T., Taniguchi, E., Fukasawa, K., Machida, T., Oki, H., Arai, T., Ichikawa, K., Hasako, S., Haze, K., Kodera, T., Kawanishi, N., Takahashi-Suzuki, I., Nakatsuru, Y., Kotani, H., and Iwasawa, Y., *Cell Cycle*, 2010, vol. 15, pp. 1590–1600.
- Fry, D., Bedford, D.C., Harvey, P.H., Fritsch, A., Keller, P.R., Wu, Z., Dobrusin, E., Leopold, W.R., Fattaey, A., and Garrett, M.D., *J. Biol. Chem.*, 2001, vol. 18, pp. 16617–16623.
- Molecular Operating Environment (MOE), C.C.G.I., 1010 Sherbooke St. West, Suite #910, Montreal, QC, Canada, H3A 2R7, 2013. https://www.chemcomp.com/MOE-Molecular_Operating_Environment.htm. Accessed January 4, 2018.
- Sanders, M.P., Barbosa, A.J., Zarzycka, B., Nicolaes, G.A., Klomp, J.P., de Vlieg, J., and del Rio, A., *J. Chem. Inf. Model.*, 2012, vol. 52, pp. 1607–1620.
- <https://www.ebi.ac.uk/chembl/>.
- Lipinski, C.A., Lombardo, F., Dominy, B.W., and Feeney, P.J., *Adv. Drug Deliv. Rev.*, 2001, vol. 46, pp. 3–26.
- Feixiong, C., Weihua, L., Yadi, Z., Jie, S., Zengrui, W., Guixia, L., Philip, W.L., and Yun, T., *J. Chem. Inf. Model.*, 2012, vol. 52, pp. 3099–3105.
- <https://www.rcsb.org/structure/2w9z>.
- <https://www.rcsb.org/structure/5L2I>.
- Simon-Szabó, L., Kokas, M., Greff, Z., Boros, S., Bánhegyi, P., Zsákai, L., Szántai-Kis, C., Vantus, T., Mandl, J., Bánhegyi, G., Vályi-Nagy, I., Örfi, L., Ullrich, A., Csala, M., and Kéri, G., *Bioorg. Med. Chem. Lett.*, 2016, vol. 26, p. 424.
- Kraker, A.J., Hartl, B.G., Amar, A.M., Barvian, M.R., Showalter, H.D., and Moore, C.W., *Biochem. Pharmacol.*, 2000, vol. 60, p. 885.
- Chen, L., Yap, J.L., Yoshioka, M., Lanning, M.E., Fountain, R.N., Raje, M., Scheenstra, J.A., Strovel, J.W., and Fletcher, S., *ACS Med. Chem. Lett.*, 2015, vol. 6, p. 764.
- Tan, L., Akahane, K., McNally, R., Reyskens, K.M., Ficarro, S.B., Liu, S., Herter-Sprue, G.S., Koyama, S., Pattison, M.J., Labella, K., Johannessen, L., Akbay, E.A., Wong, K.K., Frank, D.A., Marto, J.A., Look, T.A., Arthur, J.S., Eck, M.J., and Gray, N.S., *J. Med. Chem.*, 2015, vol. 58, p. 16:6589.
- <https://pubchem.ncbi.nlm.nih.gov/>.